International Journal of Biochemistry and Cell Biology 117 (2019) 105624

Contents lists available at ScienceDirect

International Journal of Biochemistry and Cell Biology

journal homepage: www.elsevier.com/locate/biocel

L-DOPA causes mitochondrial dysfunction *in vitro*: A novel mechanism of L-DOPA toxicity uncovered

Steven Giannopoulos[a], Kate Samardzic[a], Benjamin B.A. Raymond[b], Steven P. Djordjevic[b], Kenneth J. Rodgers[a,*]

[a] Neurotoxin Research Group, School of Life Sciences, Faculty of Science, University of Technology Sydney, Australia
[b] I3 institute, School of Life Sciences, Faculty of Science, University of Technology Sydney, Australia

ARTICLE INFO

Keywords:
L-dopa
Parkinson's disease
Mitochondrial dysfunction
Non-protein amino acid

ABSTRACT

In Parkinson's disease (PD), as in many other neurodegenerative disorders, mitochondrial dysfunction, protein misfolding, and proteotoxic stress underly the disease process. For decades, the primary symptomatic treatment for PD has been the dopamine precursor L-DOPA (Levodopa). L-DOPA however can initiate protein misfolding through its ability to mimic the protein amino acid L-tyrosine, resulting in random errors in aminoacylation and L-DOPA becoming mistakenly inserted into the polypeptide chain of proteins in place of L-tyrosine.

In the present study we examined the impact that the generation of DOPA-containing proteins had on human neuroblastoma cell (SH-SY5Y) function *in vitro*. We showed that even in the presence of antioxidants there was a significant accumulation of cytosolic ubiquitin in DOPA-treated cells, an upregulation in the endosomal-lysosomal degradation system, deleterious changes to mitochondrial morphology and a marked decline in mitochondrial function.The effects of L-DOPA on mitochondrial function were not observed with D-DOPA, the stereoisomer of L-DOPA that cannot be inserted into proteins so did not result from oxidative stress. We could fully protect against these effects by co-treatment with L-tyrosine, supporting the view that misincorporation of L-DOPA into proteins contributed to these cytotoxic effects, leading us to suggest that co-treatment with L-tyrosine could be beneficial therapeutically.

1. Introduction

Parkinson's disease (PD) is an age-related neurodegenerative disorder characterised by the selective loss of dopaminergic neurons in the substantia nigra pars compacta (SNpc) of the midbrain resulting in a deficiency in nigral dopaminergic neurotransmission (Surmeier, 2018). For decades, the primary symptomatic treatment for PD has been the dopamine precursor L-3,4-dihydroxyphenylalanine (L-DOPA or levodopa). At the time of PD diagnosis, it is estimated that between 50% and 70% of dopaminergic neurons within the SNpc have degenerated (Giguere et al., 2018), but by increasing the supply of exogenous L-DOPA, the synthesis of dopamine can be increased in the surviving dopaminergic neurons. A neuropathological hallmark of these remaining neurons is the cytoplasmic and axonal accumulation of insoluble proteins known collectively as Lewy bodies, of which fibrillar aggregates of misfolded α-synuclein are a major component (Halliday et al., 2008). Only 5–10% of patients have a monogenic form of PD, so the vast majority of cases are multifactorial in their aetiology (Scott et al., 2017). Analyses of the monogenic forms of PD have allowed key disease-associated pathways to be identified. Genetic mutations in the Parkin and PTEN-induced kinase 1 (PINK1) genes are common, both of which are crucial in regulating oxidative phosphorylation in the electron transport chain and in maintaining mitochondrial quality control (Bogaerts et al., 2008). Thus, mitochondrial dysfunction has been implicated as a possible cause of dopaminergic neuron loss in PD (Larsen et al., 2018). Mitochondria are critical to neuronal function and supply energy for synaptic activity and calcium buffering after depolarization (Bingol and Sheng, 2016). Polymorphisms in complex 1 are known to be susceptibility factors for sporadic PD, and compounds that inhibit mitochondrial complex 1 can produce parkinsonian-like symptoms in

Abbreviations: DMEM, Dulbecco's minimal essential medium; BCA, Bicinchoninic acid; BSA, Bovine serum albumin; DAPI, 4′,6-Diamidine-2′-phenylindole dihydrochloride; DA, dopamine; EMEM, Eagle's medium essential medium; FCS, foetal calf serum; D-DOPA, D-3,4-dihydroxyphenylalanine; L-DOPA, L-3,4-dihydroxyphenylalanine; LAMP1, Lysosomal-associated membrane protein 1; TyrRS, Tyrosyl-tRNA Synthetase; OCR, Oxygen consumption rate; PBS, Phosphate buffered saline; PD, Parkinson's disease; ROS, Reactive oxygen species; SNpc, Substantia nigra pars compacta; SOD, superoxide dismutase; TCA, trichloroacetic acid

* Corresponding author at: School of Life Sciences, Faculty of Science, University of Technology Sydney, Australia.
E-mail address: kenneth.rodgers@uts.edu.au (K.J. Rodgers).

https://doi.org/10.1016/j.biocel.2019.105624
Received 16 April 2019; Received in revised form 26 September 2019; Accepted 30 September 2019
Available online 22 October 2019
1357-2725/

animal models (Valente et al., 2004; Blesa and Przedborski, 2014). In addition, a number of PD genes have been identified that encode components of the ubiquitin-proteasome pathway; F-box only protein 7 (Fbxo7) and α-synuclein (Abdel-Salam, 2014). So, in PD, as in many other neurodegenerative diseases, mitochondrial function, protein folding and proteotoxic stress are a fundamental part of the disease process.

L-DOPA itself has been shown to initiate protein misfolding *in vitro* since it is a close structural analogue of the proteinogenic amino acid L-tyrosine (Rodgers and Dean, 2000). The structural similarity of these two molecules is such that L-DOPA can be incorporated into cell proteins in place of L-tyrosine (Ozawa et al., 2005). This phenomenon occurs *via* a protein synthesis-dependent pathway, where the amino and carboxyl groups participate in peptide bonding so that L-DOPA is inserted into the polypeptide backbone of newly synthesised proteins (Rodgers et al., 2002, 2004, 2006). This phenomenon of protein amino acid 'mimicry' is now well understood even at the level of tRNA synthetase activation (Song et al., 2017). The post-mitotic status of neurons makes these cells highly susceptible to non-native, damaged or misfolded proteins (Lee et al., 2006), thus a progressive accumulation of modified L-DOPA-containing proteins over many years of L-DOPA treatment could contribute to an accelerated neuronal dysfunction in PD.

In the present study we examined the impact the generation of DOPA-containing proteins could have on cell function *in vitro*. Although DOPA is inherently a reactive molecule, the ability of L-DOPA to cause oxidative stress to cells in culture is largely an artifact due to the high oxygen concentrations (~20%) to which the cells are exposed, as well as the presence of metal ions in the culture medium (Clement et al., 2002). To protect cells from oxidative stress in culture we supplemented the culture medium with antioxidants. We showed that even in the presence of antioxidants there was a significant accumulation of cytosolic ubiquitin aggregates, an upregulation in the lysosomal system, deleterious changes to mitochondrial morphology and a marked decline in mitochondrial function. We could fully protect against these effects by co-treatment with L-tyrosine supporting the view that misincorporation of L-DOPA into proteins contributes to these cytotoxic effects.

2. Materials and methods

2.1. Chemicals and reagents

All experiments were conducted using the SH-SY5Y human neuroblastoma cell line purchased from the American Type Culture Collection (ATCC, Manassas, VA, USA). Catalase from bovine liver, superoxide dismutase (SOD) from bovine liver, L-3,4-Dihydroxyphenylalanine (L-DOPA), L-tyrosine, Triton X-100, bovine serum albumin (BSA), fetal bovine serum (FBS), Dulbecco's Modified Eagle's Medium (DMEM), Eagle's Minimum Essential Medium (EMEM), anti-rabbit IgG H + l goat polyclonal secondary antibody (cat. no. 20010) and 4′,6-Diamidine-2′-phenylindole dihydrochloride (DAPI) were from Sigma-Aldrich Co. (St. Louis, MO, USA).

D-3,4-Dihydroxyphenylalanine (D-DOPA) was from Toronto Research Chemicals Inc. (Toronto, Ontario, Canada). Anti-Mouse IgG H + L goat polyclonal secondary antibody (cat. no. 18772) was from Biotium Inc. (Fremont, CA, USA). Anti-ubiquitin rabbit polyclonal antibody (cat. no. ab7780), anti-mitochondria mouse monoclonal antibody (cat. no. ab3298) and anti- LAMP1 mouse monoclonal antibody (cat. no. ab25630) were purchased from Abcam Inc. (Cambridge, MA, USA). L-glutamine and trypsin-ethylenediaminetetraacetic acid (EDTA) were from Gibco Life Sciences (Carlsbad, CA, USA). Potassium phosphate monobasic anhydrous and glycine were from Amresco Inc. (Solon, Oh, USA). Phosphate Buffered Saline (PBS) was from Astral Scientific (Taren Point, NSW, Australia) and Vectashield fluorescent anti-fade reagent was from Vector Laboratories Inc. (Burlingame, CA, USA).

2.2. Cell culture

SH-SY5Y cells were maintained in 175 cm^2 flasks containing DMEM medium supplemented with 10% heat-inactivated FBS and 2 mM L-glutamine in a 37 °C humidified atmosphere of 5% CO_2. When cell cultures reached 75–80% confluency adherent cells were detached and harvested *via* TrypLE (Thermo Fisher, MA, USA) incubation for 5 min at 37 °C. The cell suspension was centrifuged at 1000 × *g* for 5 min and subcultured in 1 in 4 ratios. During experimentation, cell cultures that reached confluency were harvested and centrifuged at 1000 × *g* for 5 min. The cell pellet was resuspended in fresh DMEM medium and aspirated through an 18-gauge needle secured to a 10 ml syringe to homogenise cells in medium. Cell count was conducted using a hemocytometer while being visualised under a Nikon Eclipse Ts2 inverted light microscope (Olympus Co., Tokyo, Japan). Cells were then subsequently plated in 12-well plates containing 15 mm round glass coverslips at a population density of 1×10^5 cells per well and allowed to equilibrate overnight (16 h) in DMEM media (1 ml per well) before treatments. For this study, SH-SY5Y cells did not exceed a passage number higher than 35.

2.3. Preparation of reagents for cell culture

SOD and catalase were prepared in 50 mM and 0.1 M potassium phosphate buffer respectively at pH 7.5, to final activities of 100 units/ml each. L-tyrosine stock was prepared in 0.5 M hydrochloric acid. L-DOPA and D-DOPA stocks were prepared in 18 ml water from a Milli-Q filtration system (Millipore). For experiments, all solutions used were sterilised by passing through a Minisart® 0.2 µm Luer Lock syringe filter (Sigma-Aldrich, St. Louis, MO, USA) and diluted to the final culture concentrations in EMEM medium supplemented with 10% heat-inactivated FBS and 2 mM L-glutamine. All reagents and complete medium were warmed to 37 °C before use.

2.4. Cell culture and treatment conditions

Prior to each treatment, DMEM medium was removed from each well and replaced with 1 ml of EMEM medium alone or supplemented with various concentrations of either D- or L-DOPA and incubated for 24 h. Experiments involving antioxidants were conducted by co-incubating untreated and DOPA treated cells with catalase (100 units/ml) and SOD (100 units/ml) antioxidants. All L-tyrosine competition studies were conducted by co-incubating L-DOPA treated and untreated cells with 10 mM L-tyrosine, catalase (100 units/ml) and SOD (100 units/ml). Directly following all treatments, cells were washed three times in PBS, and cell fixed by flooding with 4% paraformaldehyde in PBS for 30 min at room temperature.

2.5. Immunofluorescence

Following fixation, cells were flushed with 100 mM glycine and incubated for 5 min to quench excess aldehydes. Subsequently, cells were blocked with a BSA blocking solution (2% BSA w/v in PBS) and incubated for 1 h. Cells to be stained for mitochondrial and LAMP1 components were permeabilised in 0.5% Triton X-100 diluted in PBS for 5 min. Cells were then separately stained for ubiquitin, mitochondrial and LAMP1 components. Cells stained for ubiquitin were incubated with the primary ubiquitin rabbit polyclonal antibody (ab7780) at 1:2000 dilution in 2% BSA for 1 h. Cells stained for LAMP1 were incubated with the primary LAMP1 mouse monoclonal antibody at 1:200 dilution in 2% BSA for 1 h. Cells stained for mitochondria were incubated with the primary mitochondrial mouse monoclonal antibody (ab3298) at 1:500 dilution in 0.5% Triton X-100 diluted in 2% BSA for 24 h at 4 °C. All experimentation from this point forward was conducted

in the dark to prevent photo bleaching of the fluorescent antibodies. Subsequently, these cells were incubated with their corresponding green (CF488) secondary fluorescent antibodies. Cells stained with the primary ubiquitin antibody were incubated with the secondary fluorescent anti-rabbit polyclonal antibody (18772) at 1: 1000 dilution in 2% BSA for 1 h. Cells stained with the primary mitochondrial and primary LAMP1 antibodies were incubated with the secondary fluorescent anti-mouse polyclonal antibody (20010) at 1:1000 dilution in 2% BSA for 1 h. Once staining with primary and secondary antibodies was complete, all cells were then stained for their nuclei components with DAPI at 0.05 μg/ml in PBS for 5 min. Subsequently, coverslips were removed from their respective well and left to dry. 3 μL of Vectashield anti-fade reagent was then added to each coverslip and affixed to glass microscope slides, followed by securing coverslips to slides using nail varnish. Note: all cells were rinsed three times with PBS between each of the treatments listed and a volume of 500 μL solution used per well for each treatment, likewise all incubations were performed at room temperature unless otherwise stated.

2.6. Microscopy and cell measurements

The LAMP1 and ubiquitin components stained with green secondary fluorescent antibodies were visualised using an Olympus BX51 Upright Research Fluorescent Microscope (Olympus Co., Tokyo, Japan) equipped with an NIBA filter unit in the green spectrum (λ_{ex}470-495 nm) and the corresponding nuclei stained with fluorescent DAPI conjugate were visualised using the NUA filter unit in the blue spectrum range (λ_{ex}360-370 nm). The fluorescent images were captured at 20x magnification, photographed using the phase Olympus DP70 colour camera (Olympus Co.) operated by cellSens software version 1.16 (Olympus Co.). Super-resolution 3D images of mitochondria and DAPI stained components were acquired using the DeltaVision™ OMX SR Microscope (GE Healthcare., Buckinghamshire, UK) equipped with a 60x/1.42 NA PlanApo oil immersion lens (Olympus Co.). Mitochondria were visualised in the green (λ_{ex}488 nm) and DAPI in the blue colour range (λ_{ex}405 nm) and images captured using the One sCMOS OMX camera (GE Healthcare). Super-resolution images were processed using the OMX Acquisition Control software version 3.70.9220 (GE Healthcare) and images reconstructed using the SoftWoRx software version 6.5.2 (GE Healthcare).

Cellular ubiquitin, LAMP1 and DAPI components were imaged at 350 ms, 2 s and 80 ms exposure times respectively in all experiments. The total fluorescence intensity of LAMP1 and ubiquitin components were recorded by measuring the fluorescence signal emission of each image after thresholding, with a constant 1000 units of background elimination in LAMP1 images. Cellular fluorescence intensity was then normalised to the total number of DAPI stained nuclei, counted using imageJ software with thresholding. The super-resolution mitochondrial images were analysed and five unique shape descriptors measured including mitochondrial: 1) surface area, 2) perimeter (mitochondrial size), 3) aspect ratio [(major axis)/(minor axis)] reflecting the length-to-width ratio or degree of mitochondrial elongation; 4) form factor [(perimeter2)/(4π x surface area)] reflecting the complexity and branching of mitochondria, and 5) circularity [4 x (surface area/perimeter2)] where values range from 1 to zero, whereby a value of 1 indicates a perfect sphere and values approaching zero indicate less spherical and more elongated shape (Picard et al., 2013). All quantitative measurements were performed using the public domain NIH ImageJ software version 1.41 (developed at the United States National Institutes of Health and available at http://rsb.info.nih.gov/ij).

2.7. Cell viability assay

Cells were plated in 96 well plates at a population density of 30,000 cells/ well, allowed to adhere overnight, and then treated in triplicate with the following concentrations of L-DOPA; 50 μM, 100 μM, 200 μM, 500 μM and 1000 μM with or without SOD (100 U/ml) and catalase (100 U/ml) antioxidants. Cells were treated for 24 h and then subsequently incubated with 10% Alamar Blue cell viability reagent (Thermo Fisher) for 2 h. Fluorescence was read at λ_{ex} 570/em 585. Protein concentration was determined with the BCA assay (Smith et al., 1985) and samples were normalised for protein concentration.

2.8. Amino acid competition

Cell viability was also measured in the presence of L-DOPA in conjunction with L-tyrosine. 10 mM L-tyrosine and 100 U/ml catalase and SOD antioxidants were added to EMEM amino acid deficient media. The amino acid supplemented EMEM was then co-incubated with 1000 μM L-DOPA for 24 h. Cell viability was measured using the Alamar Blue assay and normalised to protein concentration using the BCA assay.

2.9. Mitochondrial bioenergetics assay

The mitochondrial bioenergetics analysis was performed by measuring the oxygen consumption rate (OCR) of cultured cells using the Seahorse Xfe24 Extracellular Flux analyser (Agilent, Santa Clara, CA, USA). Cells were plated at a population density of 30,000 cells/well and left overnight to adhere. Cells were then subsequently treated with L-DOPA at a concentration of 100 μM for 24 h. The Mito Stress Test (Agilent) was then performed according to the manufacturer's instructions. Cells were then washed in Seahorse assay media, prepared using the manufacturer's protocol and kit reagents (oligomycin (1 μM), FCCP (1 μM) and antimycin A/rotenone (0.5 μM)). OCR values were normalised to protein concentration using the BCA assay. Basal respiration, maximal respiration, ATP production, non-mitochondrial respiration and proton leak were then calculated using the Seahorse XF Cell Mito Stress Test Report Generator. Calculations were as follows: non-mitochondrial respiration equates to the minimum rate measurement after antimycin A/rotenone injection; basal respiration equates to last rate measurement before oligomycin injection minus non-mitochondrial respiration; maximal respiration equates to maximum rate measurement after FCCP injection minus non-mitochondrial respiration; ATP production equates to last rate measurement before oligomycin injection minus the minimum rate after oligomycin injection

2.10. JC-10 mitochondrial membrane potential assay

Mitochondrial membrane potential was measured using the JC-10 Microplate Assay Kit (Abcam) according to the manufacturer's instructions. SH-SY5Y were cultured overnight in a 96-well plate at a population density of 30,000 cells/ well in DMEM. Cells were then treated with 200 μM LDOPA in the presence of catalase (100 U/ml) and SOD (100 U/ml) antioxidants in EMEM for 24 h. At the end of the treatment period the treatment media was replaced with phenol red free EMEM and 50 μl of JC-10 dye-loading solution was added to each well. After a 30 min incubation in a 37 °C, 5% CO_2 incubator, 50 μl of Assay Buffer B was added to each well. Fluorescence intensity was then measured at Ex/Em = 490/525 nm and Ex/Em = 540/590 nm. The change in mitochondrial membrane potential was measured as the ratio between red aggregate (Em = 590 nm) and green monomeric forms (Em = 525 nm) of JC-10. Increasing ratios indicate mitochondrial membrane depolarisation. Representative images were captured in the FITC and TRITC channels with a high-speed charge-coupled device (CCD) camera using the NIS-Elements acquisition software mounted on a Nikon Ti inverted fluorescence microscope equipped with 20X objective lens (Plan Apo NA 1.4 aperture).

2.11. Statistical analysis

All sample (cell) treatments were carried out in triplicate. All results were expressed as the mean plus or minus standard error of the mean

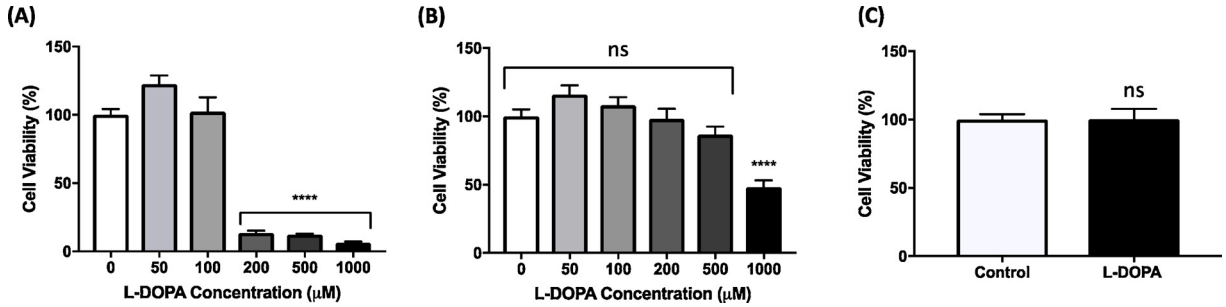

Fig. 1. Toxicity of L-DOPA in the presence and absence of antioxidants and L-tyrosine. SH-SY5Y cells viability was tested using the Alamar Blue assay following incubation with L-DOPA for 24 h in medium alone (A), and in the presence of SOD (100 U/ml) and catalase (100 U/ml) (B). A further viability test was conducted on SH-SY5Y cells exposed to SOD (100 U/ml), catalase (100 U/ml) and 10 mM L-tyrosine in the presence or absence of 1000 μM L-DOPA (C). All culture experiments were performed in triplicate. Results are expressed as mean values and error bars represent standard error of the mean. Statistical analysis was conducted using one-way ANOVA with Dunnett's multiple comparisons test (A and B), while unpaired *t*-test was used in results shown in (C) represented by **** ($p < 0.0001$) and * ($p < 0.05$) and ns (not statistically significant).

(SEM). Statistical analysis was conducted using two-tailed Student's *t*-tests and one-way ANOVA with Dunnett's multiple comparisons tests and significance inferred if $p < 0.05$. All results were graphed and statistical analysis conducted using the GraphPad Prism 7 software version 7.0 (CA, USA).

3. Results

3.1. L-DOPA exposure results in a decrease in cell viability that can be prevented using a combination of antioxidants and L-tyrosine supplementation

To examine the degree of cytotoxicity caused by L-DOPA, we exposed SH-SY5Y cells to a range of L-DOPA concentrations (0–1000 μM) for 24 h and assessed cell viability using the Alamar Blue assay. Significant cytotoxic effects were demonstrated at L-DOPA concentrations of 200 μM and above, with more than an 80% loss in viability occurring (Figure 1, 2, 3, 4, ig. 5 and 6A). As L-DOPA is known to exert cytotoxicity through both L-DOPA-mediated oxidative stress and proteotoxic stress *via* its misincorporation into nascent cell proteins, we set out to differentiate the effects on cell viability attributed to both mechanisms of toxicity. To determine the degree to which L-DOPA-mediated oxidative stress was responsible for the cytotoxic effects seen, we exposed SH-SY5Y cells to the same L-DOPA concentrations (0–1000 μM) in the presence of the antioxidants SOD (100 U/ml) and catalase (100 U/ml). This combination of antioxidants has previously been shown to protect against L-DOPA mediated oxidative stress *in vitro* (Chan et al., 2012). Co-administration of the antioxidants was fully protective at all L-DOPA concentrations below 1000 μM (Fig. 1B) as indicated by no significant loss in cell viability. However, at 1000 μM L-DOPA, there was a 50% loss in viability. To confirm that this loss in viability was due to the misincorporation of L-DOPA into proteins, we additionally supplemented the culture medium with 10 mM L-tyrosine, which resulted in no loss of viability (Fig. 1C).

3.2. L-DOPA treatment results in the accumulation of ubiquitinylated proteins in cells

To examine the effect that L-DOPA has on the proteome, we visualised and quantified the levels of ubiquitin in SH-SY5Y cells following treatment with 200 μM D-DOPA or 200 μM L-DOPA for 24 h. To identify effects that were specifically related to oxidative stress we employed the D-isomer of DOPA in this study since it can form the same reactive oxygen species as the L-isomer but, is not utilised in protein synthesis by mammalian cells. In L-DOPA-treated cells, ubiquitin-positive fluorescent staining was increased around 4-fold relative to control cells and around 1.7-fold relative to D-DOPA treated cells (Fig. 2a and b). To establish that the additional ubiquitin staining observed in L-DOPA, but not D-DOPA treated cells, was not due to oxidative stress we combined the previous treatments with the antioxidants SOD (100 U/ml) and catalase (100 U/ml). In the presence of the antioxidants there was no increase in ubiquitin staining in D-DOPA-treated cells compared to control cells, demonstrating that the previous upregulation in ubiquitin staining seen in the D-DOPA treatment was due only to oxidative stress (Fig. 2a and b). Even in the presence of antioxidants however, L-DOPA-treated cells still exhibited a 2-fold increase in ubiquitin staining compared to the control cells, indicating that this effect could be due to the misincorporation of L-DOPA into proteins and independent of oxidative stress. This was further substantiated by showing that this increase in ubiquitin staining was prevented by the addition of L-tyrosine (10 mM) to the culture medium (Fig. 2a and b).

3.3. L-DOPA treatment results in an increase in LAMP1 staining in cells

To determine if the increased ubiquitin staining in cells was also associated with changes to the autophagy-lysosomal system, we treated SH-SY5Y cells with 200 μM D-DOPA or 200 μM L-DOPA for 24 h and stained for LAMP1, a glycoprotein present on the membrane of lysosomes. As lysosomes are vesicles responsible for digesting damaged cellular organelles and biomolecules as a mechanism of cell quality control, changes in LAMP1 abundance allows us to quantify the relative level of internal cellular damage with each respective treatment condition. In L-DOPA-treated cells, LAMP1 fluorescent staining was increased 4-fold relative to control cells (Fig. 3a and b) and 1.5-fold relative to that in D-DOPA treated cells. To determine if the additional LAMP1 staining seen in the L- but not D-DOPA treated cells was independent of oxidative stress we co-administered the DOPA treatments with antioxidants. In the presence of the antioxidants SOD (100 U/ml) and catalase (100 U/ml) there was no increase in LAMP1 staining in D-DOPA-treated cells compared to control cells (Fig. 3a and b). Even in the presence of antioxidants, L-DOPA-treated cells exhibited a 2-fold increase in LAMP1 staining compared to the control cells but this increase in LAMP1 staining was prevented by adding L-tyrosine (10 mM) to the culture medium (Fig. 3a and b).

3.4. L-DOPA-treatment results in mitochondrial fragmentation

As mitochondrial dysfunction has been recognised as a key pathological hallmark in neurodegenerative disorders we set out to investigate the extent to which L-DOPA-treatment impacts mitochondrial morphology in mammalian cells. Following treatment of SH-SY5Y cells with 200 μM D- or L-DOPA for 24 h, we stained cells with an antibody to mitochondrial proteins, and identified changes to mitochondrial morphology by quantifying various shape descriptors using ImageJ

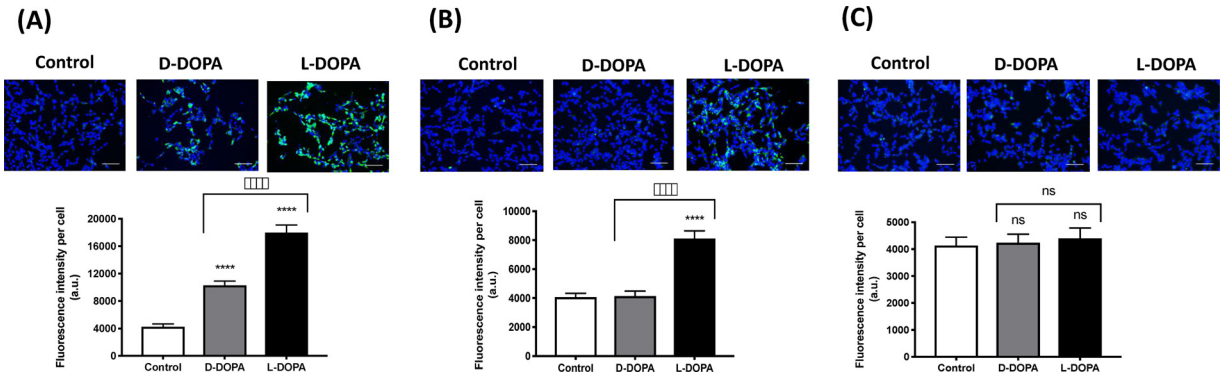

Fig. 2. Ubiquitin staining of D-DOPA and L-DOPA treated cells. SH-SY5Y cells were cultured for 24 h in medium alone or medium supplemented with 200 μM D-DOPA or L-DOPA (A), and with the addition of SOD (100 U/ml) and catalase (100 U/ml) (B), and with addition of SOD (100 U/ml), catalase (100 U/ml) and 10 mM L-tyrosine (C). Fluorescent images of antibody stained ubiquitin were captured in the green spectrum (lex470-495 nm) and nuclei stained with DAPI in the blue spectrum (lex360-370nm). Scale bars denote a 50 μm length. Fluorescence intensity was quantified and normalised to the number nuclei in the field.Results are expressed as mean values and error bars represent standard error of the mean for results obtained from triplicate experiments (n = 3). Statistical analysis was conducted using unpaired t-tests and significance represented as ****($p < 0.0001$) relative to control and •••• ($p < 0.0001$) comparing D-DOPA and L-DOPA and ns (not statistically significant). (For interpretation of the references to colour in this figure legend, the reader is referred to the web version of this article.)

software on super resolution microscopy images captured using a DeltaVision™OMX SR microscope (Fig. 4). We chose to incorporate measurements of form factor and aspects ratio to provide indications of mitochondrial elongation and complexity of morphology. Conversely, the use of circularity provides information about the sphericity of the mitochondria. Collectively, the use of these shape descriptors provides strong indications of the degree of mitochondria exhibiting deleterious, fragmented morphologies, which correlate to more spherical and less elongated/complex morphologies. Mitochondria are naturally long, elongated/branched structures, which allows for the maintenance of correct membrane potential and translocation of molecules such as oxygen and ions along its length for adequate ATP production, thus alteration of this natural morphology results in mitochondrial dysfunction (Mancuso et al., 2007).

In this study, there were no significant changes in mitochondrial morphology evident in D-DOPA-treated cells compared to control cells (Fig. 4). However, mitochondrial shape descriptors differed significantly in L-DOPA-treated cells compared to control and D-DOPA-treated cells, with significant increases in mitochondrial circularity and surface area, and corresponding decreases in mitochondrial elongation/complexity (form factor and aspect ratio) (Fig. 4), indicating that L-DOPA exposure induced substantial mitochondrial dysfunction in these cells. Also, in control cultures around 13% of cells had fragmented mitochondria in contrast, 80% of cells had fragmented mitochondria in the L-DOPA treated cultures.

The antioxidants SOD (100 U/ml) and catalase (100 U/ml) were unable to protect against the deleterious mitochondrial morphological changes induced by L-DOPA treatment, indicating that the mechanism of mitochondrial toxicity was independent of oxidative stress. (Fig. 4B). However, with the addition of L-tyrosine, none of the deleterious changes in mitochondrial morphology were evident in L-DOPA-treated cells (Fig. 4C).

3.5. L-DOPA-treatment results in a decline in mitochondrial function

To further investigate the deleterious effects of L-DOPA on mitochondrial morphology that were shown to be independent of oxidative stress (Fig. 4), we examined changes in mitochondrial function in the presence of L-DOPA and antioxidants. The mitochondrial bioenergetics profile in L-DOPA-treated and control cells was quantified using the Seahorse Xfe24 Extracellular Flux analyser. In SH-SY5Y cells exposed to 100 μM L-DOPA for 24 h in medium containing SOD (100 U/ml) and catalase (100 U/ml) there was a 28% reduction in maximal respiration (Fig. 5B) and a 48% reduction in basal respiration (Fig. 5D)

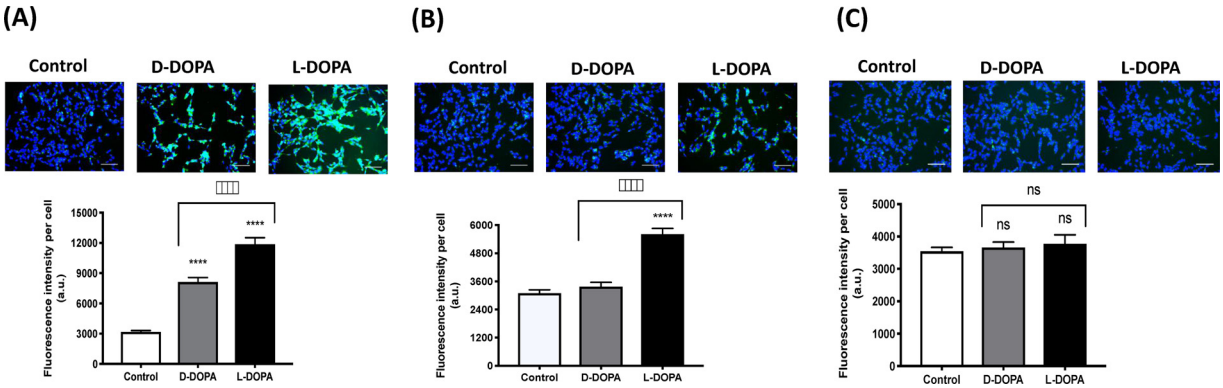

Fig. 3. LAMP1 Staining of D-DOPA and L-DOPA treated cells. SH-SY5Y cells were cultured for 24 h in medium alone or medium supplemented with 200 μM D-DOPA or L-DOPA (A), and with the addition of SOD (100 U/ml) and catalase (100 U/ml) (B), and with addition of SOD (100 U/ml), catalase (100 U/ml) and 10 mM L-tyrosine (C). Fluorescent images of antibody stained LAMP1 were captured in the green spectrum (lex470-495 nm) and nuclei stained with DAPI in the blue spectrum (lex360-370 nm). Scale bars denote a 50 μm length. Fluorescence intensity was quantified and normalised to the number nuclei in the field. Results are expressed as mean values and error bars represent standard error of the mean for results obtained from triplicate experiments (n = 3). Statistical analysis was conducted using unpaired t-tests and significance represented as ****($p < 0.0001$) relative to control and •••• ($p < 0.0001$) comparing D-DOPA and L-DOPA and ns (not statistically significant). (For interpretation of the references to colour in this figure legend, the reader is referred to the web version of this article.)

(A)

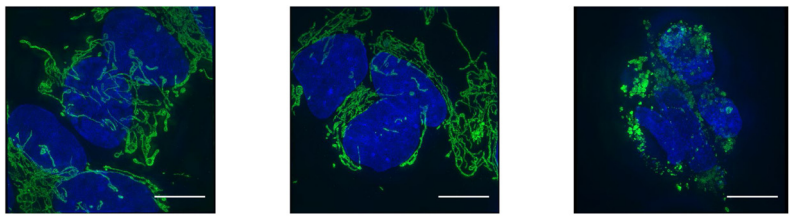

	Control	D-DOPA	p-value (C-D)	L-DOPA	p-value (C-L)	p-value (D-L)
Surface Area (μm^2)	0.237 +/- 0.008	0.254 +/- 0.008	0.136	0.332 +/- 0.009	<0.0001	<0.0001
Perimeter (μm)	2.612 +/- 0.064	2.675 +/- 0.065	0.495	2.105 +/- 0.037	<0.0001	<0.0001
Circularity (0-1)	0.530 +/- 0.005	0.527 +/- 0.005	0.628	0.766 +/- 0.005	<0.0001	<0.0001
Aspect Ratio	2.598 +/- 0.030	2.558 +/- 0.028	0.329	1.704 +/- 0.011	<0.0001	<0.0001
Form Factor	2.737 +/- 0.047	2.713 +/- 0.046	0.707	1.578 +/- 0.025	<0.0001	<0.0001

(B)

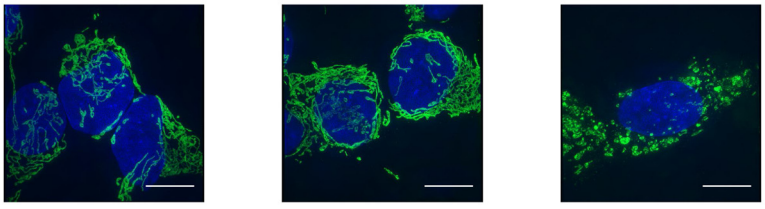

	Control	D-DOPA	p-value (C-D)	L-DOPA	p-value (C-L)	p-value (D-L)
Surface Area (μm^2)	0.224 +/- 0.009	0.229 +/- 0.008	0.678	0.318 +/- 0.010	<0.0001	<0.0001
Perimeter (μm)	2.521 +/- 0.077	2.514 +/- 0.063	0.946	2.317 +/- 0.047	<0.0001	<0.0001
Circularity (0-1)	0.519 +/- 0.006	0.525 +/- 0.005	0.493	0.707 +/- 0.005	<0.0001	<0.0001
Aspect Ratio	2.569 +/- 0.038	2.538 +/- 0.034	0.533	1.878 +/- 0.017	<0.0001	<0.0001
Form Factor	2.757 +/- 0.059	2.675 +/- 0.046	0.271	1.680 +/- 0.020	<0.0001	<0.0001

Fig. 4. Visualisation and morphological analysis of mitochondria. Super resolution fluorescent images of mitochondria in SH-SY5Y cells. Images were captured following 24 h incubation in medium alone (control), or with the addition of 200 μM D- DOPA or L-DOPA **(A)**; following 24 h incubation in medium supplemented with SOD (100 U/ml) and catalase (100 U/ml), with the addition of 200 μM D-DOPA or L-DOPA **(B)**; or following 24 h incubation in medium supplemented with SOD (100 U/ml), catalase (100 U/ml) and 10 mM L-tyrosine, with the addition of 200 μM D- DOPA or L-DOPA **(C)**. Super-resolution fluorescent images of antibody stained mitochondria were captured using an OMX SR microscope in the green spectrum range (λex488 nm) and nuclei stained with DAPI in the blue spectrum range (λex405 nm). The morphology of over 1000 mitochondria were analysed using ImageJ software. Results are expressed as mean values with standard error of the mean for the results obtained from triplicate experiments (n = 3) and statistical analysis conducted using unpaired *t*-test. The scale bars denote a 10 μm length. (For interpretation of the references to colour in this figure legend, the reader is referred to the web version of this article).

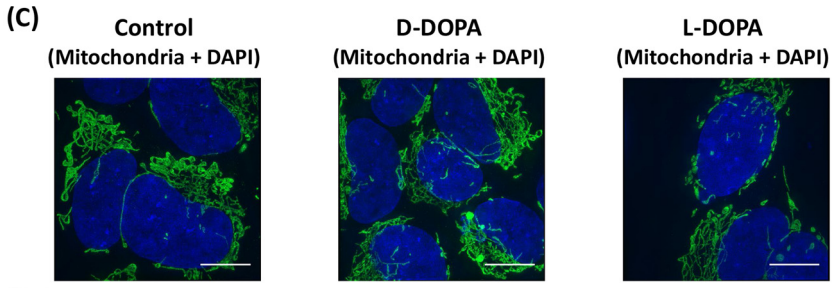

	Control	D-DOPA	p-value (C-D)	L-DOPA	p-value (C-L)	p-value (D-L)
Surface Area (μm^2)	0.248 +/- 0.012	0.247 +/- 0.012	0.976	0.266 +/- 0.013	0.315	0.294
Perimeter (μm)	2.572 +/- 0.090	2.604 +/- 0.090	0.800	2.647 +/- 0.096	0.565	0.740
Circularity (0-1)	0.534 +/- 0.007	0.530 +/- 0.007	0.690	0.544 +/- 0.008	0.350	0.189
Aspect Ratio	2.539 +/- 0.044	2.526 +/- 0.043	0.833	2.517 +/- 0.046	0.724	0.879
Form Factor	2.590 +/- 0.061	2.649 +/- 0.061	0.494	2.574 +/- 0.066	0.864	0.409

Fig. 4. (*continued*)

compared to control cells. Basal respiration is the oxygen consumption used to meet the cellular ATP demand under baseline conditions and maximal respiration is the maximal oxygen consumption rate attained following the addition of the uncoupler FCCP. The mitochondria of cells treated with L-DOPA also exhibited a 44% reduction in proton leak (Fig. 5F) and 49% reduction in ATP synthesis (Fig. 5E) compared to control cells. The measure of ATP production is derived from the decrease in oxygen consumption following oligomycin injection and shows the portion of basal respiration used to drive mitochondrial ATP production, while proton leak refers to remaining basal respiration not

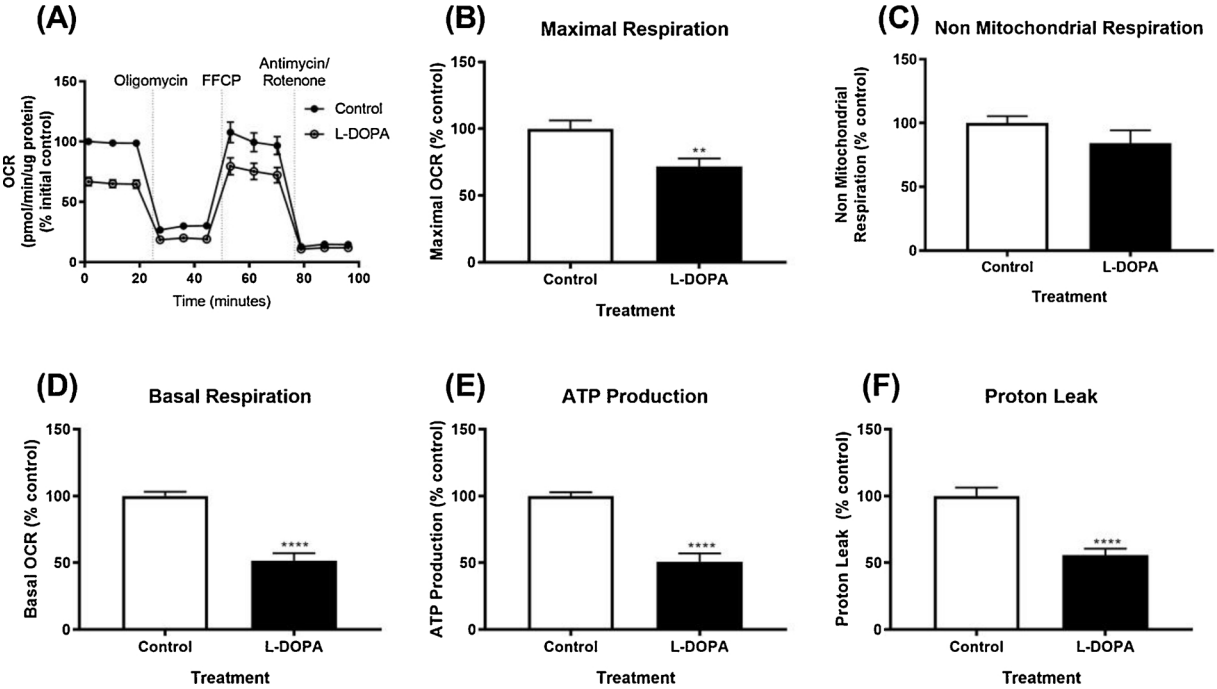

Fig. 5. Analysis of mitochondrial bioenergetics. Mitochondrial bioenergetics were examined in SH-SY5Y cells following L-DOPA treatment in the presence of antioxidants. Cells were incubated in medium containing SOD (100 U/ml) and catalase (100 U/ml) (control) or in the same media containing 100 μM L-DOPA for 24 h. Panel A shows oxygen consumption rate (OCR) over the course of the experiment normalised to protein concentration, panel B shows maximal respiration, panel C shows non-mitochondrial respiration, panel D shows basal respiration, panel E shows ATP production and panel F shows proton leak. Results are expressed as mean values and error bars represent standard error of the mean for results obtained from triplicate experiments (n = 3). Statistical analysis was conducted using unpaired t-tests and significance represented as ** ($p < 0.01$), ****($p < 0.0001$).

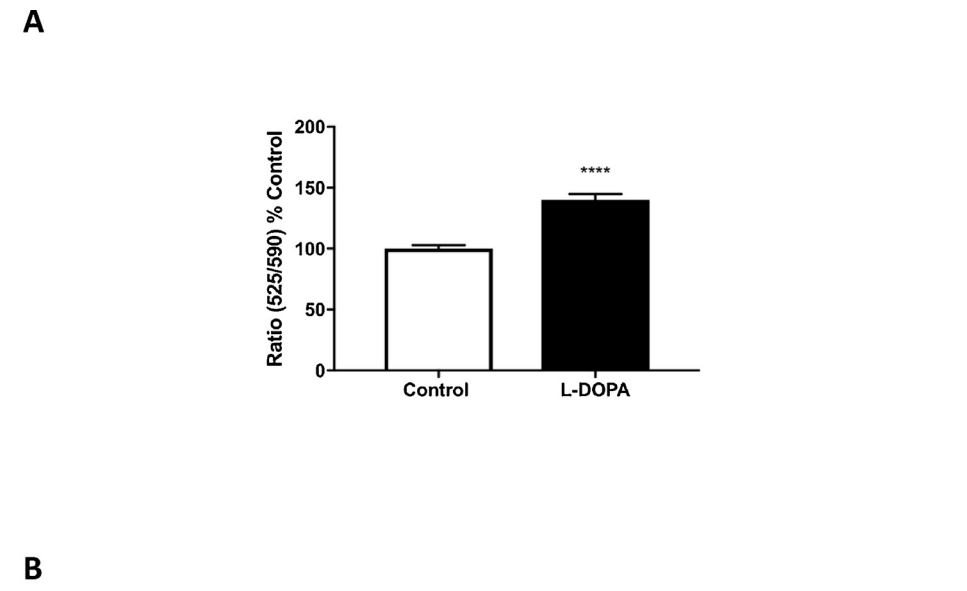

Fig. 6. Analysis of mitochondrial membrane potential. Mitochondrial membrane potential was determined in SH-SY5Y cells using JC-10 staining. Cells were incubated in medium supplemented with SOD (100 U/ml) and catalase (100 U/ml) and in the same medium containing 200 μM L-DOPA for 24 h. Fluorescent microplate measurements of mitochondrial membrane potential are expressed as a ratio of JC-10 monomer/aggregate (525/590 nm) (**6A**). Data represents percentage of control cells (set at 100%) as mean values, error bars represent standard error of the mean from results obtained from triplicate experiments (n = 3) and statistical analysis was conducted using unpaired *t*-test with **** representing $p < 0.0001$. **6B** shows representative images of JC-10 aggregate and monomeric staining for the control (top panels) and L-DOPA (bottom panels) treated cells.

coupled to ATP production.

To further determine the extent of mitochondrial dysfunction induced by L-DOPA we assessed the mitochondrial membrane potential in cells exposed to 200 μM L-DOPA in the presence of SOD (100 U/ml) and catalase (100 U/ml) for 24 h. It was shown that in cells exposed to L-DOPA there was a significant decrease in mitochondrial membrane potential (Fig. 6A). This is represented visually by the images of the monomeric and aggregate forms of JC-10 (Fig. 6B). The healthy, respiring control cells show increased JC-10 sequestered aggregate within the mitochondrial matrix (red fluorescence). Conversely, L-DOPA treated cells demonstrate lower aggregate and more monomeric form (green fluorescence) caused by JC-10 leaking out of the mitochondrial matrix and into the cytosol, indicating significant loss in mitochondrial membrane potential.

4. Discussion

It has been shown that some non-encoded amino acids can 'mimic' protein amino acids by replacing them in protein synthesis (Song et al., 2017; Rodgers and Shiozawa, 2008; Rodgers, 2014). Azetidine-2-carboxylic acid (Aze), for example, is not rejected by the prolyl tRNA synthetase ProRS editing system and can be incorporated into some proline positions in the protein sequence *in vitro* and *in vivo* (Song et al., 2017). In previous studies we have shown that L-DOPA can replace the protein amino acid, L-tyrosine, in protein synthesis (Rodgers et al., 2004, 2006; Rodgers et al., 2002; Ozawa et al., 2005), and in the present studies we provide evidence that incorporation of L-DOPA into proteins can have a profound effect on specific aspects of cell function *in vitro*.

Using the Alamar Blue assay, a sensitive measure of cell function and cytotoxicity (Rampersad 2012), we showed that L-DOPA was toxic to mammalian cells at concentrations as low as 200 μM (Fig. 1). In the

presence of antioxidants however, significant cytoxicity was only detectable at 1000 μM DOPA (Fig. 2) highlighting the importance of oxidative stress in L-DOPA toxicity *in vitro*. In cell culture, oxidative stress is greatly enhanced due to the high oxygen concentrations (~20%) to which the cells are exposed, along with the presence of relatively high concentrations of metal ions in the culture medium (Clement et al., 2002). A second mechanism of L-DOPA toxicity relates to its ability to mimic L-tyrosine and cause protein aggregation due to the generation of non-native proteins containing peptide-bonded DOPA (Dunlop et al., 2008). A combination of two antioxidants (catalase and SOD) can fully protect cells from L-DOPA-mediated oxidative stress in cell culture allowing the toxicity arising from L-DOPA incorporation into proteins to be selectively examined (Chan et al., 2012). The toxicity resulting from L-DOPA incorporation into proteins can also be determined by comparing L-DOPA toxicity to that of its enantiomer D-DOPA, which can be taken up by cells, form similar reactive species as L-DOPA (for review (Rodgers and Dean, 2000)), but cannot be incorporated into proteins by mammalian cells. In addition, increasing the concentration of L-tyrosine in the medium will outcompete L-DOPA at the level of TyrRS charging and prevent incorporation of L-DOPA into proteins. All of these strategies were used in the present studies to specifically identify the impact that L-DOPA incorporation into proteins has on cell function *in vitro*.

In the Alamar Blue viability assay a component of L-DOPA toxicity was due to incorporation into protein; antioxidants were only partially protective but with the addition of L-tyrosine, cells were fully protected against L-DOPA toxicity. In the presence of antioxidants, 1000 μM DOPA was required to produce a significant decrease in cell viability. Significant changes in protein turnover and mitochondrial morphology and function however were detectable at concentrations as low as 100–200 μM. When we examined ubiquitin staining as an indicator of damaged or non-native protein accumulation in cells we found that the two-fold increase in ubiquitin staining caused by D-DOPA was completely prevented by antioxidants so could be attributed to oxidative stress. L-DOPA caused a four-fold increase in ubiquitin staining relative to control cells but, in contrast to D-DOPA-treated cells, this increase was only reduced by around 50% in the presence of antioxidants. The addition of an excess of L-tyrosine along with the antioxidants fully protected against the accumulation of ubiquitinylated proteins in cells; these data are consistent with L-DOPA causing protein or organelle damage through its ability to be mistakenly incorporated into proteins. It should be noted that this marked increase in ubiquitin staining was observed at only 200 μM DOPA. In order to examine this further we looked for changes in the autophagy-lysosomal system which maintains homeostasis by removing damaged proteins or organelles. The increased production of LAMP1 glycoproteins in L-DOPA treated cells supported the view that the autophagic system was responding to damaged proteins or damaged organelles. Consistent with our previous data we showed that the presence of D-DOPA (200 μM) resulted in an increase in LAMP1 staining due only to oxidative stress, whereas in L-DOPA treated cells a component of the toxicity was resistant to antioxidants and could therefore be attributed to incorporation into protein and was prevented by the addition of L-tyrosine.

Non-protein amino acid (NPAA) incorporation into proteins and the resulting modification to proteins can perturb mitochondrial function. For example, canavanine, a non-encoded amino acid and arginine mimic, disturbed mitochondrial protein homeostasis by affecting the folding of proteins synthesised in the mitochondria as well as those imported from the cytosol (Konovalova et al., 2015). In the present studies we observed profound changes to mitochondrial shape by examining super-resolution images of cells exposed to L-DOPA (200 μM). Quantitative analysis indicated extensive mitochondrial fragmentation and swelling. Previous studies have shown that under stressful conditions, mitochondria undergo excessive fission reactions leading to mitochondrial fragmentation and dysfunction (Zorov et al., 2019). D-DOPA treated cells did not exhibit any evidence of changes to mitochondrial shape even in the absence of antioxidants suggesting, somewhat unexpectedly, that the mechanism of mitochondrial damage was unrelated to oxidative stress. Again, L-tyrosine supplementation was fully protective, supporting L-DOPA incorporation into protein as the mechanism of mitochondrial damage as was demonstrated for the NPAA canavanine (Konovalova et al., 2015). The basal level of tyrosine in the culture medium was 459 μM but the addition of 10 mM tyrosine fully prevented L-DOPA toxicity (Fig. 1C), increased staining for ubiquitin and LAMP1 (Figs. 2 and 3) and mitochondrial changes (Figs. 4–6). In all cases the medium used for control cells was also supplemented with 10 mM tyrosine. Mitochondrial bioenergetic analysis confirmed that L-DOPA, even at 100 μM, significantly impaired mitochondrial respiration and ATP production. In these studies, catalase (100 U/ml) and SOD (100 U/ml) were present in the culture medium confirming that the mechanism of damage was unrelated to oxidative stress (Fig. 5). This assay was more sensitive and required the concentration of L-DOPA to be reduced from 200 μM to 100 μM. This functional change was supported by studies showing that L-DOPA (200 μM) induced mitochondrial depolarization, indicating disruption to the mitochondrial membrane potential caused by the uneven distribution of ions across the inner mitochondrial membrane (Fig. 6).

Taken together these data demonstrate that L-DOPA is capable of damaging mitochondria by a mechanism unrelated to oxidative stress. Mitochondria are comprised of around 1000 proteins that, with the exception of 13, are nuclear encoded, translated in the cytosol and the precursor proteins imported into the mitochondria (Backes and Herrmann, 2017). The imported proteins generally require proteolytic processing and chaperone assisted folding before they can assume their native conformation (Backes and Herrmann, 2017). Even intermittent protein misfolding as could occur due to DOPA-incorporation could cause proteotoxic stress in the mitochondria and cause a decline in function as observed in the present studies. The protection afforded by supplementing the culture media with L-tyrosine and the lack of toxicity of D-DOPA strongly support the view that the damage to mitochondria is due to the misincorporation of L-DOPA into proteins. The misincorporation of L-DOPA into protein by protein synthesis has been shown to occur both *in vitro* and *in vivo* (Rodgers et al., 2002, 2004). L-DOPA caused a decline in mitochondrial function at concentrations as low as 100 μM, which is approximately 4-fold the peak plasma concentration of L-DOPA reported in PD patients (Dizdar et al., 1999). Mitochondrial dysfunction is closely linked to the pathophysiology of PD and since preservation of remaining SNcDA neurons is critical to slow the progression of the disease in L-DOPA treated patients, these *in vitro* data would support the view that L-DOPA should be taken with L-tyrosine supplementation to prevent the accelerated accumulation of cytosolic protein aggregates and to prevent irreversible damage to mitochondria. Many of the early studies investigating diet and L-DOPA therapy that supported limiting dietary protein intake were conducted on small populations. More recently Virmani and colleagues carried out a comprehensive study and concluded that clinically significant protein interaction might occur only in a small subset of PD patients with earlier disease onset and those with familial form of the disease (Pincus and Barry, 1987; Cereda et al., 2010). In principle if L-tyrosine is being used to protect against the damaging effects of L-DOPA it should be effective at comparable concentrations to L-DOPA since it is the native substrate for TyrRS so will have a higher affinity for the enzyme.

A marked reduction in complex I activity in the mitochondrial electron transport chain has been reported in PD patients, specifically in areas of the brain relevant to PD (Schapira, 2008, 2012; Schapira et al., 1998). This could be secondary to L-DOPA treatment since chronic administration of L-DOPA, at levels usually employed therapeutically, caused a marked reduction in complex I activity in rat brains but no significant changes in the activities of complex II and complex IV (Przedborski et al., 1993). While these findings suggest that the deleterious effects of levodopa could be specific to complex I, in some cell lines (NB69) complex IV activity has been reported to be the most

sensitive to L-DOPA (Pardo et al., 1995). The *in vitro* effects on complex IV activity in NB69 cells however were mediated by oxidative stress and sensitive to ascorbic acid so might result from the hyperoxic conditions of cell culture and not be representative of the *in vivo* effects (Pardo et al., 1995). Using electron microscopy, we reported changes to mitochondrial morphology in L-DOPA but not in D-DOPA-treated neuroblastoma cells (SH-SY5Y) consistent with observations in the present study that some deleterious effects of L-DOPA on mitochondria are not mediated by oxidation (Chan et al., 2012). Damaged mitochondria can release cytochrome c into the cytosol activating pro-apoptotic pathways (pedrosa and Soares da silva 2002) with activation of caspase 3 and increased expression of markers of apoptosis (Dunlop et al., 2011).

After 50 years of use, L-DOPA remains the most effective therapy for the treatment of PD. The degree to which L-DOPA itself causes neurodegeneration has been the subject of ongoing debate. We postulate that the effects of L-DOPA on mitochondrial function have been overlooked; protection with co-administration of L-tyrosine however could be a practical solution and could help better preserve the remaining dopaminergic neurons.

References

Abdel-Salam, O.M., 2014. The paths to neurodegeneration in genetic Parkinson's disease. CNS Neurol. Disord. Drug Targets 13, 1485–1512.

Backes, S., Herrmann, J.M., 2017. Protein translocation into the intermembrane space and matrix of mitochondria: mechanisms and driving forces. Front. Mol. Biosci. 4, 83.

Bingol, B., Sheng, M., 2016. Mechanisms of mitophagy: PINK1, Parkin, USP30 and beyond. Free Radic. Biol. Med. 100, 210–222.

Blesa, J., Przedborski, S., 2014. Parkinson's disease: animal models and dopaminergic cell vulnerability. Front. Neuroanat. 8, 155.

Bogaerts, V., Theuns, J., van Broeckhoven, C., 2008. Genetic findings in Parkinson's disease and translation into treatment: a leading role for mitochondria? Genes Brain Behav. 7, 129–151.

Cereda, E., Barichella, M., Pedrolli, C., Pezzoli, G., 2010. Low-protein and protein-redistribution diets for Parkinson's disease patients with motor fluctuations: a systematic review. Mov. Disord. 25, 2021–2034.

Chan, S.W., Dunlop, R.A., Rowe, A., Double, K.L., Rodgers, K.J., 2012. L-DOPA is incorporated into brain proteins of patients treated for Parkinson's disease, inducing toxicity in human neuroblastoma cells in vitro. Exp. Neurol. 238, 29–37.

Clement, M.V., Long, L.H., Ramalingam, J., Halliwell, B., 2002. The cytotoxicity of dopamine may be an artefact of cell culture. J. Neurochem. 81, 414–421.

Dizdar, N., Granerus, A.K., Hannestad, U., Kullman, A., Ljungdahl, A., Olsson, J.E., Kagedal, B., 1999. L-dopa pharmacokinetics studied with microdialysis in patients with Parkinson's disease and a history of malignant melanoma. Acta Neurol. Scand. 100, 231–237.

Dunlop, R.A., Brunk, U.T., Rodgers, K.J., 2011. Proteins containing oxidized amino acids induce apoptosis in human monocytes. Biochem. J. 435, 207–216.

Dunlop, R.A., Dean, R.T., Rodgers, K.J., 2008. The impact of specific oxidized amino acids on protein turnover in J774 cells. Biochem. J. 410, 131–140.

Giguere, N., Burke Nanni, S., Trudeau, L.E., 2018. On cell loss and selective vulnerability of neuronal populations in Parkinson's disease. Front. Neurol. 9, 455.

Halliday, G., Hely, M., Reid, W., Morris, J., 2008. The progression of pathology in longitudinally followed patients with Parkinson's disease. Acta Neuropathol.

Konovalova, S., Hilander, T., Loayza-Puch, F., Rooijers, K., Agami, R., Tyynismaa, H., 2015. Exposure to arginine analog canavanine induces aberrant mitochondrial translation products, mitoribosome stalling, and instability of the mitochondrial proteome. Int. J. Biochem. Cell Biol. 65, 268–274.

Larsen, S.B., Hanss, Z., Kruger, R., 2018. The genetic architecture of mitochondrial dysfunction in Parkinson's disease. Cell Tissue Res. 373, 21–37.

Mancuso, C., Scapagini, G., Curro, D., Giuffrida Stella, A.M., De Marco, C., Butterfield, D.A., Calabrese, V., 2007. Mitochondrial dysfunction, free radical generation and cellular stress response in neurodegenerative disorders. Front. Biosci. 12, 1107–1123.

Ozawa, K., Headlam, M.J., Mouradov, D., et al., 2005. Translational incorporation of L-3,4-dihydroxyphenylalanine into proteins. FEBS J. 272, 3162–3171.

Pardo, B., Mena, M.A., de Yebenes, J.G., 1995. L-dopa inhibits complex IV of the electron transport chain in catecholamine-rich human neuroblastoma NB69 cells. J. Neurochem. 64, 576–582.

Picard, M., White, K., Turnbull, D.M., 2013. Mitochondrial morphology, topology, and membrane interactions in skeletal muscle: a quantitative three-dimensional electron microscopy study. J. Appl. Physiol. 114 (1985), 161–171.

Pincus, J.H., Barry, K.M., 1987. Plasma levels of amino acids correlate with motor fluctuations in parkinsonism. Arch. Neurol. 44, 1006–1009.

Przedborski, S., Jackson-Lewis, V., Muthane, U., Jiang, H., Ferreira, M., Naini, A.B., Fahn, S., 1993. Chronic levodopa administration alters cerebral mitochondrial respiratory chain activity. Ann. Neurol. 34, 715–723.

Rodgers, K.J., 2014. Non-protein amino acids and neurodegeneration: the enemy within. Exp. Neurol. 253, 192–196.

Rodgers, K.J., Dean, R.T., 2000. The metabolism of protein-bound DOPA in mammals. Int. J. Biochem. Cell Biol. 32, 945–955.

Rodgers, K.J., Hume, P.M., Dunlop, R.A., Dean, R.T., 2004. Biosynthesis and turnover of DOPA-containing proteins by human cells. Free Radic. Biol. Med. 37, 1756–1764.

Rodgers, K.J., Hume, P.M., Morris, J.G., Dean, R.T., 2006. Evidence for L-dopa incorporation into cell proteins in patients treated with levodopa. J. Neurochem. 238, 29–37.

Rodgers, K.J., Shiozawa, N., 2008. Misincorporation of amino acid analogues into proteins by biosynthesis. Int. J. Biochem. Cell Biol. 40, 1452–1466.

Rodgers, K.J., Wang, H., Fu, S., Dean, R.T., 2002. Biosynthetic incorporation of oxidized amino acids into proteins and their cellular proteolysis. Free Radic. Biol. Med. 32, 766–775.

Schapira, A.H., 2008. Mitochondria in the aetiology and pathogenesis of Parkinson's disease. Lancet Neurol. 7, 97–109.

Schapira, A.H., 2012. Targeting mitochondria for neuroprotection in Parkinson's disease. Antioxid. Redox Signal. 16, 965–973.

Schapira, A.H., Gu, M., Taanman, J.W., Tabrizi, S.J., Seaton, T., Cleeter, M., Cooper, J.M., 1998. Mitochondria in the etiology and pathogenesis of Parkinson's disease. Ann. Neurol. 44, S89–98.

Scott, L., Dawson, V.L., Dawson, T.M., 2017. Trumping neurodegeneration: Targeting common pathways regulated by autosomal recessive Parkinson's disease genes. Exp. Neurol. 298, 191–201.

Song, Y., Zhou, H., Vo, M.N., et al., 2017. Double mimicry evades tRNA synthetase editing by toxic vegetable-sourced non-proteinogenic amino acid. Nat. Commun. 8, 2281.

Surmeier, D.J., 2018. Determinants of dopaminergic neuron loss in Parkinson's disease. FEBS J.

Valente, E.M., Abou-Sleiman, P.M., Caputo, V., et al., 2004. Hereditary early-onset Parkinson's disease caused by mutations in PINK1. Science 304, 1158–1160.

Zorov, D.B., Vorobjev, I.A., Popkov, V.A., et al., 2019. Lessons from the discovery of mitochondrial fragmentation (Fission): a review and update. Cells 8.